

# Ridged Waveguide Filter Optimization Using the Neural Networks and a Modified Simplex Method

Mohamed Yahia, Jun W. Tao, Hafedh Benzina and Mohamed N. Abdelkrim

**Abstract**—The rectangular ridged waveguide filter optimization is discussed. To improve the performances of the optimized filters, we exploit the height of the gaps between the ridges and the waveguide wall. We propose a hybrid technique, constituted by the artificial neural networks (ANNs) and the circuit theory. The proposed approach is applied to the design of four-pole and six-pole narrow band-pass filters. The results agree well with those produced by conventional simulators.

**Index Terms**— Rectangular ridged waveguides, filter optimization, multimodal variational method, artificial neural networks.

## I. INTRODUCTION

The rectangular ridged waveguides are particularly important for the design of a number of passive microwave components for spatial applications (i.e. filters, tapers...) by virtue of their large bandwidth and low characteristic impedance.

In [1] and [2] rectangular ridged waveguide filter optimization is performed. The generalized scattering matrices (GSMs) are obtained using the multidimensional variationnal method (MVM) [1]. However, only the lengths of the waveguides are optimized. The exploitation of the height of the gaps between the ridges and the waveguide wall increases the performances of the ridged waveguide filter and permits to get narrower relative bandwidth (BW). However, the optimization process becomes very time-consuming because a new simulation for every change in the height of the gaps is needed. This feature makes ANNs very useful tool because they produce accurate and instantaneous responses.

In [3] a multilayer perceptron neural network (MLPNN) model is established to determine the characteristic parameters of quadruple-ridged square waveguides. Reference [4] reviews the state-of-the-art microwave filter modeling, optimization and design methods using ANN techniques.

Manuscript received March 11, 2010.

M. Yahia is with LAPLACE, ENSEEIHT, MACS and ENIG (e-mail:mohamed\_yahia1@yahoo.fr).

J.W. Tao is with Laboratoire Plasma et Conversion d'Energie (LAPLACE), ENSEEIHT, 2 rue Camichel 31071 Toulouse cedex France tao@laplace.univ-tls.fr).

H. Benzina is with the national engineering school of Gabès (ENIG), Rue Omar Ibn Elkhattab 6029 Gabès Tunisia (e-mail: hafed.benzina@ieee.org)

Mohamed N. Abdelkrim is with Unité de recherche Modélisation, Analyse et Commande de système (MACS), ENIG, Rue Omar Ibn Elkhattab 6029 Gabès Tunisia (e-mail : naceur.abdelkrim@enig.rnu.tn).

In this paper, we propose a hybrid approach to the design of rectangular ridged waveguide filter. The proposed neuromodel to be used for the design of the microwave circuit is presented in a decomposed manner, where the GSMs of the waveguide discontinuities are generated by a MLPNN which are later connected by the circuit theory. The optimized parameters are the lengths of the waveguides and the height of the gaps between the ridges and the waveguide wall. Due to the complex input-output relation and in order to avoid local minima, conventional optimization tools need generally a first order starting point provided by the circuit theory [1] and [2]. To surmount this problem, we apply a modified simplex method presented in [5] to filter optimization in very narrow bandwidth. No starting points are required. We apply the proposed model to the design of four-pole and six-pole narrow band-pass filters. The results will be compared to those produced by conventional full-wave FEM based CAD tools. All simulations are developed in Matlab on a PC (Intel CPU 1.66 GHz with 1-GB RAM).

## II. CLASSICAL OPTIMIZATION METHOD

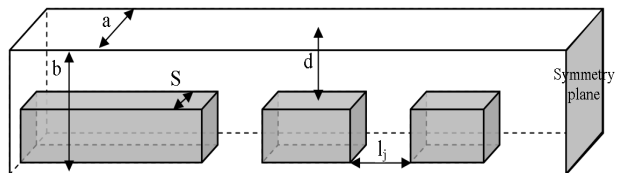


Fig. 1 Geometries of a four pole waveguide filter.  $a=8$  mm  $b=3.8$  mm  $S=3.6$  mm,  $d=0.8$  mm,  $i=\{1..6\}$ ,  $j$ : variable  $j=\{1..9\}$ .

We consider a four pole rectangular ridged waveguide as shown in fig. 1. The fundamental modes in the ridged and the rectangular waveguides have cut-off frequencies equal to  $f_{c_{rid}}=9.0363$  GHz and  $f_{c_{rec}}=18.75$  GHz, respectively. The MVM is applied to generate the GSMs of the discontinuities in the waveguide filter and the response of the complete circuit is obtained by connecting all the GSMs through the respective waveguides as in [1] and [2]. To obtain the desired performances, we minimize the following objective function:

$$U = \sum_i |S_{11}(L, f_i)| + (1 - |S_{12}(L, f_i)|) \\ + \sum_j |S_{12}(L, f_j)| + (1 - |S_{11}(L, f_j)|) \quad (1)$$

$f_i$  and  $f_j$  correspond to the sample frequencies within the

pass-band and the stop-band respectively and  $L$  is the vector containing all the waveguide lengths to be optimized. The optimization process is a modified simplex method [5] which can produce good performances even in narrow BW. Due to geometry symmetry, half parameters are optimized. We use one accessible mode in the ridged waveguide and three accessible modes in the rectangular waveguides.

#### A. Four-pole ridged waveguide filter optimization

We take two examples of four-pole band-pass filters. The first filter (F1) is 28.57%BW with a central frequency  $f_0=13.125\text{GHz}$ . The second filter (F2) is 10.9%BW with a central frequency  $f_0=14.225\text{GHz}$ .

$l_1$ (mm)	$l_2$ (mm)	$l_3$ (mm)	$l_4$ (mm)	$l_5$ (mm)
1.029	2.873	3.185	1.400	4.184

TABLE I. OPTIMIZED PARAMETERS OF THE FILTER F1 USING THE MVM.

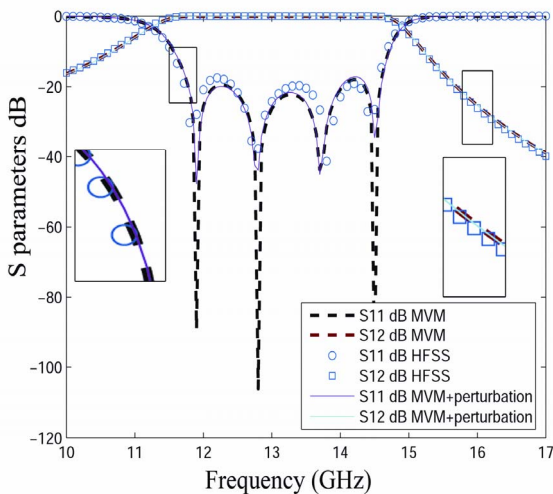


Fig. 2. Variation of S11 dB and S12 dB of the filter F1 with respect to the frequency.

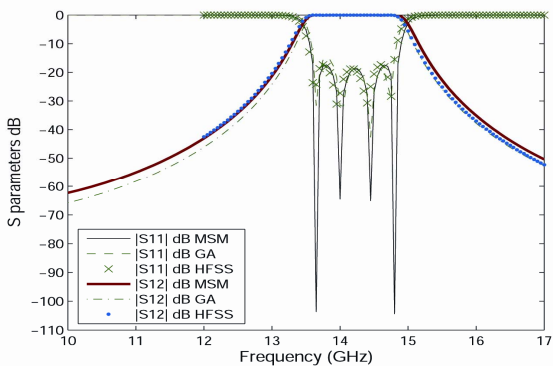


Fig. 3. Variation of S11 dB and S12 dB of the filter F2 with respect to the frequency.

TABLE II. OPTIMIZED PARAMETERS OF THE FILTER F2 USING THE MVM.

	$l_1$ (mm)	$l_2$ (mm)	$l_3$ (mm)	$l_4$ (mm)	$l_5$ (mm)
MSM	2.36126	0.73293	7.55263	0.09229	8.77503
GA	2.511742	0.665166	7.8865	0.09	9.03914

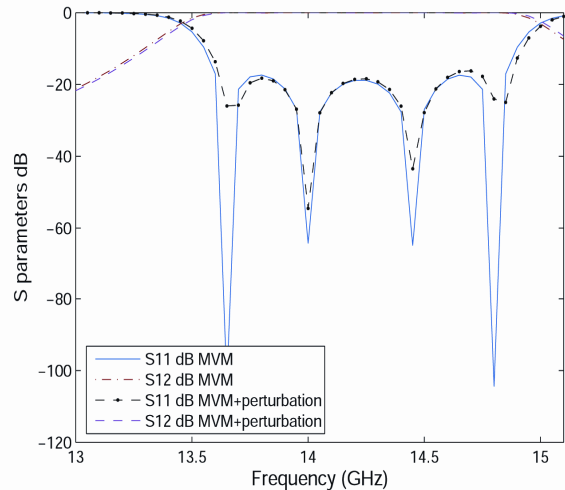


Fig. 4. Response of the filter F2 using the original and the perturbed optimized parameters.

Table I presents the optimized parameters of the filter F1 using the MVM. Fig. 2 shows the responses of the optimized filter. We get no difficulties to obtain the desired response using the SM as an optimizer. We observe good agreement with the results produced by the full-wave FEM based CAD tool (i.e. HFSS). To test the stability of the minimum, we add a small perturbation to the optimized parameters. The rectangular waveguide lengths have been increased by  $10 \mu\text{m}$  while those of resonators are decreased by  $10 \mu\text{m}$ . No obvious deterioration of filter the performances is observed because the optimized parameters are sufficiently large with respect to the perturbation ( $\pm 10 \mu\text{m}$ ) (fig. 2).

We are interesting in the filter F2. It is very difficult to get the desired response using the SM because the BW is too small. To attain our end, we apply the MSM [5] and we compare the performances with those produced by the genetic algorithm (GA) [6] where the crossover probability (pc) ranges from 0.7 to 0.8, the mutation probability (pm) ranges from 0.08 to 0.1 and the number of individuals in the population is equal to 45.

The final optimized parameters are presented in table II. Fig. 3 displays the responses of the filter F2 using the solutions provided by the MSM and the GA. We employed the optimized parameters produced by the MSM to draw the HFSS's model. We observe that all simulations agree well. However, the CPU times of the MSM and the GA are about 10 minutes and 20 minutes, respectively.

To test stability of the minimum, we added a small perturbation to the optimized parameters. The rectangular waveguide lengths have been increased by  $10 \mu\text{m}$  while those of resonators are decreased by  $10 \mu\text{m}$ . The results are presented in fig. 4. The deterioration of filter performances is observed.

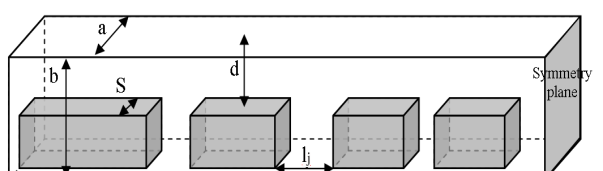


Fig. 5. Geometries of a six pole waveguide filter.  $a=8$  mm  $b=3.8$  mm  $S=3.6$ mm,  $d_i=0.8$ mm,  $i=\{1..8\}$ ,  $l_j$ : variable  $j=\{1..13\}$ .

	$l_1$ (mm)	$l_2$ (mm)	$l_3$ (mm)	$l_4$ (mm)	$l_5$ (mm)	$l_6$ (mm)	$l_7$ (mm)
MSM	1.847	1.105	6.508	0.195	8.177	0.145	8.382
GA	2.050	0.960	6.694	0.174	8.124	0.132	8.405

TABLE III. OPTIMIZED PARAMETERS OF THE FILTER F3 USING THE MVM.

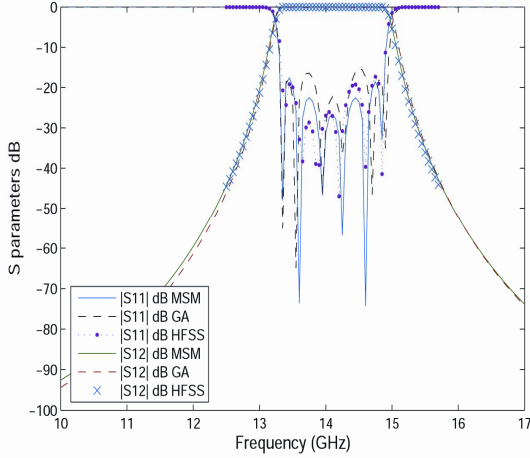


Fig. 6. Responses of the optimized filter F3 with respect to the frequency.

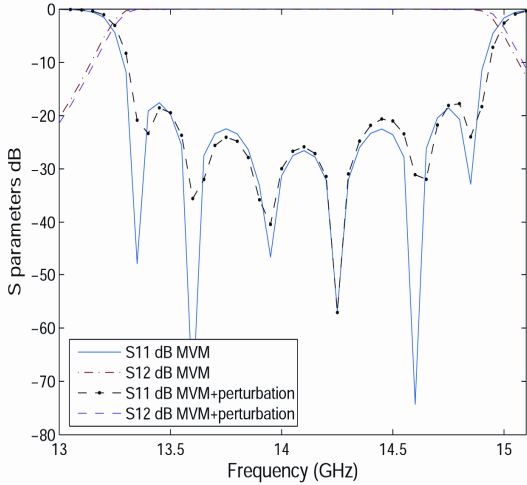


Fig. 7. Response of the filter F3 using the original and the perturbed optimized parameters.

### B. Six-pole ridged waveguide filter optimization

We consider a six-pole band-pass filter (F3) 12.38%BW with a central frequency  $f_0=14.125$ GHz (fig. 5). Table III gives the final optimized parameters using both MSM and GA with 58 individuals in the population. The HFSS's results are obtained using the final optimized parameters of the MSM shown in table III. Fig. 6 which represent the response of the filter F3 using the studied numerical methods shows that all simulations agree well. However, the CPU times of the MSM and the GA are about 25 minutes and 2 hours, respectively.

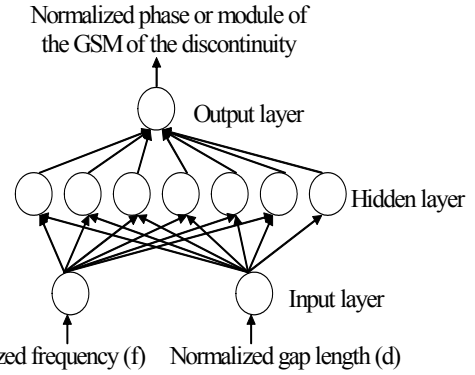


Fig. 8. Topology of the MLPNN.

To test stability of the minimum, we added a small perturbation to the optimized parameters. The rectangular waveguide lengths have been increased by 10  $\mu m$  while those of resonators are decreased by 10  $\mu m$ . The results are presented in fig. 4. The deterioration of filter performances is observed as in the filter F2. It is due to the lengths of the resonators which are not sufficiently large with respect to the perturbation ( $\pm 10 \mu m$ ). To surmount this deficiency, we optimize also the height of the gaps between the ridges and the waveguide wall. However, when repetitive simulations are required due to changes of the height of the gaps, the use of MVM is very time consuming. To overcome this deficiency, we employ the ANNs.

### III. PROPOSED NEUROMODEL OPTIMIZATION TOOL.

In this section, we employ the MLPNN which is the most popular ANN [3]. Fig. 8 shows its architecture.

#### A. Input Layer:

We use two neurons corresponding to the input parameters which are the frequency vector ( $f$ ) and height of the gap vector ( $d$ ). The cut-off frequency of the fundamental mode of the ridged waveguide  $f_{c,rid}$  changes with the eight of the gap  $d$ . The frequency ( $f$ ) ranges from  $f_{c,rid}$  to  $f_{c,rec}$ . We take 20 equidistant frequencies.  $d$  ranges from 0.6mm to 1mm with a step of 0.02mm.

#### B. Output Layer:

We use one neuron corresponding to one real parameter related to the module or the phase of the GSM's elements. The analysis of each parameter of the GSM by an independent MLPNN is easier and faster than the analysis of all parameters by single MLPNN. We use one accessible mode in the ridged waveguides and three accessible modes in the rectangular waveguides. Consequently, we have to optimize 20 upper diagonal real parameters of GSMS. Considering only fundamental modes which are propagating gives poor results.

#### C. Hidden Layer:

We choose one hidden layer with 7 neurons. The MLPNN parameters are trained with gradient descent algorithm [7]. The training samples are generated by the MVM. The training is stopped when the maximum error between the real output and the desired output is less than  $5 \cdot 10^{-3}$ . The cut-off frequency of the dominant mode in the ridged waveguides is

also generated by an independent MLPNN with one neuron in the input layer corresponding to the height of gap, 7 neurons in the hidden layer and one neuron in the output layer corresponding to the cut-off frequency. Before training, all inputs and outputs are normalized. They range from -1 to 1.

#### D. Four-pole ridged waveguide filter optimization

TABLE IV. OPTIMIZED PARAMETERS OF THE FILTER F2 USING THE NEUROMODEL.

$d_2$ (mm)	$d_3$ (mm)	$l_1$ (mm)	$l_2$ (mm)	$l_3$ (mm)	$l_4$ (mm)	$l_5$ (mm)
0.842	0.970	2.402	0.836 5	7.542	0.487	8.656

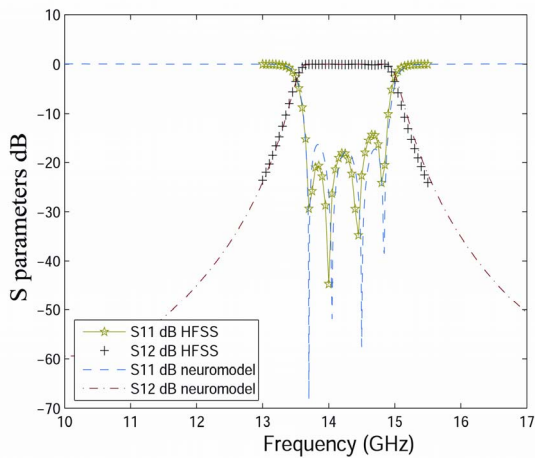


Fig. 9. Variation of S11 dB and S12 dB of the filter F2 with respect to the frequency using the proposed neuromodel.

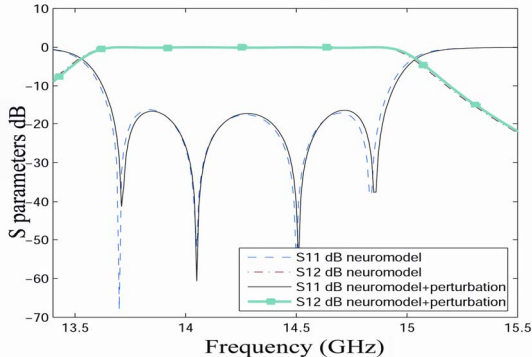


Fig. 10 Response of the filter F2 using the original and the perturbed optimized parameters using the neuromodel.

We are interesting to get the performances of the filter F2. To get the desired response, we apply the MSM as an optimizer. The optimized parameters are given in table IV. We can observe that the lengths of the resonators are not too small contrarily to those produced by the classical MVM. The optimized parameters are entered to the full-wave FEM based CAD tool (i. e. HFSS). We observe good concordance between all simulations (fig. 9).

TABLE V. OPTIMIZED PARAMETERS OF THE FILTER F3 USING THE NEUROMODEL.

$d_2$ (mm)	$d_3$ (mm)	$d_4$ (mm)	$l_1$ (mm)	$l_2$ (mm)
0.8530	0.9559	0.8978	1.91168	1.24905
$l_3$ (mm)	$l_4$ (mm)	$l_5$ (mm)	$l_6$ (mm)	$l_7$ (mm)
6.54981	0.57974	8.09129	0.35772	8.33461

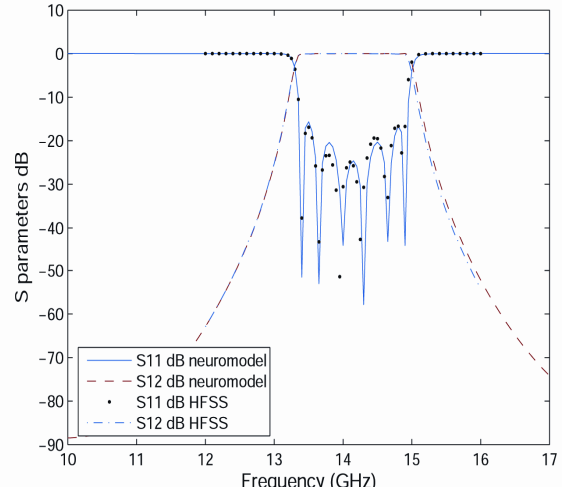


Fig. 11. Variation of S11 dB and S12 dB of the filter F3 with respect to the frequency using the proposed neuromodel.

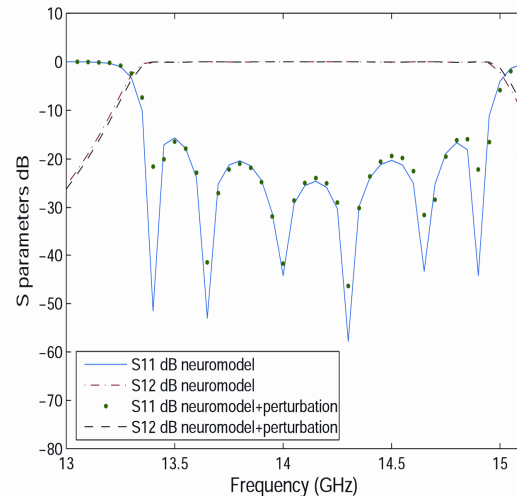


Fig. 12. Response of the filter F3 using the original and the perturbed optimized parameters using the neuromodel.

In order to test stability of the solution, the rectangular waveguide lengths have been increased by 10  $\mu\text{m}$  while those of resonators are decreased by 10  $\mu\text{m}$ . Fig. 10 shows that no obvious deterioration of the filter performances is observed because the optimized parameters are sufficiently large with respect to the 10  $\mu\text{m}$  contrarily to the minimum produced by the MVM in section II.

#### E. Six pole ridged waveguide filter optimization

We are interesting to get the performances of the filter F3. The optimized parameters obtained using the MSM are entered to the full-wave FEM based CAD tool (i. e. HFSS). We observe good concordance between all simulations (fig. 11). Fig. 12 shows that no obvious deterioration of the filter performances is observed because the optimized parameters are sufficiently large with respect to the 10  $\mu\text{m}$ .

## IV. CONCLUSIONS

We proposed a neuronal approach to improve the performances of the optimized rectangular ridged waveguide filters. The optimized parameters are the lengths of the

waveguides and the height of the gaps between the ridges and the waveguide wall. The proposed neuromodel is successfully applied to the design of four-pole and six-pole narrow band-pass filters and can easily be extended to the optimization of higher order filters. The proposed neuromodel produced minima that are more stable than the conventional optimization using the MVM.

Since 2003, he has been a Professor in Automatic Control at the National Engineering School of Gabes, Gabes, Tunisia. He is the head of the Research Unit "Modelisation, Analyse et Commande des Systèmes" "MACS".

#### REFERENCES

- [1] J. W. Tao and H. Baudrand, "Multimodal variational analysis of uniaxial waveguide discontinuities," IEEE Trans. Microwave Theory Tech., vol. 39, no. 3, pp. 506-516, Mar. 1991.
- [2] J.C. Nanan, J.W. Tao, H. Baudrand, B. Theron and S. Vigneron, "A two-step synthesis of broadband ridged waveguide bandpass filters with improved performances," IEEE Trans. Microwave Theory Tech., vol. 39, no. 12, pp.2192-2197, Dec. 1991.
- [3] Y. Tang, J. Zhao and W. Wu, "Analysis of quadruple-ridged square waveguide by multilayer perceptron neural network model," Asia-Pacific Microwave Conference, pp. 1912-1918, 2006, Yokohama.
- [4] J. E. Rayas-Sánchez, "EM-based optimization of microwave circuits using artificial neural networks: The state-of-the-Art," IEEE Trans. Microwave Theory Tech., vol. 52, no. 1, pp.420-435, Jan. 2004.
- [5] M. Yahia, J.W. Tao, H. Benzina, M.N. Abdelkrim, " Modified simplex method applied to narrow bandwidth ridged waveguide filter optimization," Mediterranean microwave symposium, pp. 1-4, Nov. 2009, Tangiers.
- [6] L L. Yin, Z. Qian , W. Hong, X. W. Zhu, Y.Chen, "The application of genetic algorithm in E-plane waveguide filter design," International Journal of Infrared and Millimetre Waves, vol. 21, no. 2, 2000.
- [7] J. W. Bandler, "Optimization methods for computer-aided design," IEEE Trans. Microwave Theory Tech., vol. 17, no. 8, pp.533-552. Aug. 1969

**Mohamed Yahia** was born in Paris, France, in 1976. He received the mastery degree in electronics and instrumentation from the Higher School of Sciences and Techniques, Tunis, Tunisia, in 2000, and the master degree in telecommunications from the Higher School of Communication, Tunis, Tunisia, in 2002. He began the Ph.D. in Electrical Engineering in the National Engineering School of Gabes, Tunisia, and the Ecole Nationale Supérieure d'Electrotechnique, d'Electronique, d'Informatique, d'Hydraulique et des Télécommunications (ENSEEIHT), Toulouse, France, in 2006.

**Junwu Tao** was born in Hubei, China, in 1962. He received the B.Sc. degree in electronics from the Department of Radio Engineering, Huazhong (Central China) University of Science and Technology, Wuhan, China, in 1982, the Ph.D. degree from the INP, Toulouse, France, in 1988, and the Habilitation degree from the University of Savoie, Chambéry, France, in 1999.

Since September 2001, he has been a full Professor at the INP, where he is engaged in the numerical methods for electromagnetism, microwave and radio-frequency components design, and microwave and millimeter-wave measurements.

**Hafed Benzina** was born in Gabes, Tunisia, in 1961. He obtained the Mastery degree in Sciences of Physics from the Faculty of Sciences, Tunis, Tunisia, in 1984, and the Ph.D. degree in microwaves electronics from the Institut National Polytechnique (INP), Toulouse, France, in 1990.

Since 1990, he is a Research Assistant with Department of Communication and Network Engineering in the National Engineering School of Gabes. His research interests include theoretical methods for solving problems of propagation in the anisotropic medias.

**Mohamed Naceur Abdelkrim** was born in Tunisia, in 1958. He received the mastery degree and the " Diplôme de Etudes Approfondies" in electrical and electronics engineering from the "Ecole Normale Supérieure de l'Enseignement Technique", Tunis, Tunisia, in 1980 and 1981, the Ph. D. and the "Doctorat d'Etat" in Automatic Control in 1985 and in 2003, both from the National Engineering School of Tunis, Tunis,Tunisia.